Solubility Parameters as Predictors of Miscibility in Solid Dispersions

DAVID J. GREENHALGH,[†] ADRIAN C. WILLIAMS,*[,†] PETER TIMMINS,[‡] AND PETER YORK[†]

Contribution from *Drug Delivery Group, Postgraduate Studies in Pharmaceutical Technology, the School of Pharmacy, University of Bradford, BD7 1DP, U.K., and Bristol-Myers Squibb, Pharmaceutical Research Institute, Moreton, Merseyside, L46 1QW, U.K..*

Received March 18, 1999. Accepted for publication July 30, 1999.

Abstract □ This paper reports interactions and possible incompatibilities in solid dispersions of hydrophobic drugs with hydrophilic carriers, with solubility parameters employed as a means of interpreting results. Systems containing ibuprofen (IB) and xylitol (XYL) in varying proportions and systems of IB with other sugars and a sugar polymer were produced using solvent evaporation and fusion methods. Additionally, bridging agents were employed with IB/XYL systems to facilitate the production of a solid dispersion. Results show that IB formed no interactions with any of the sugar carriers but interacted with all the bridging agents studied. The bridging agents were immiscible with XYL in the liquid state. Results of other reported drug/carrier systems and those from the systems studied in this paper were interpreted using Hildebrand solubility parameters. A trend between differences in drug/carrier solubility parameters and immiscibility was identified with incompatibilities evidence when large solubility parameter differences exist between drug and carrier. It was concluded that Hildebrand parameters give an indication of possible incompatibilities between drugs and carriers in solid dispersions, but that the use of partial solubility parameters may provide a more accurate prediction of interactions in and between materials and could provide more accurate indications of potential incompatibilities.

Introduction

Solid dispersions have been employed to enhance the dissolution rates of poorly water-soluble drugs, including ethenzamide,[1] nifedipine,[2,3] furosemide,[4] griseofulvin,[5,6] and tolbutamide.[6,7] However, although some amorphous dispersions are currently marketed, few solid dispersions have been developed into commercial products, due to various limitations of these systems, including physical instabilities on storage[8,9] and problems of drug/carrier immiscibility.[10,11] If the drug and the carrier are incompatible, dispersion of the drug into the carrier can be problematic, with irregular crystallization, uniformity problems, and possibly little improvement in drug dissolution rate. With a hydrophobic drug the carrier must be hydrophilic to facilitate fast dissolution of the therapeutic agent into the aqueous medium of the gastrointestinal tract. In this paper solid dispersions of ibuprofen (IB) with various sugars and polymer carriers were investigated. Results were interpreted in terms of solubility parameters, an approach which was extended to literature reports of similar systems in order to probe the applicability of this method for predicting drug/carrier compatibility.

Cohesive energy represents the total attractive forces within a condensed state material and can be defined as the quantity of energy needed to separate the atoms/molecules of a solid or liquid to a distance where the atoms or molecules possess no potential energy, i.e., no interactions occur between atoms or molecules. Further, cohesive energy density (CED) is the cohesive energy per unit volume. The CED for a material can be used to predict its solubility in other materials; if two components have similar values, they are likely to be soluble in each other, since interactions in one component will be similar to those in the other component. Thus, the overall energy needed to facilitate mixing of the constituents will be small, as the energy required to break the interactions within the components will be equally compensated for by the energy released due to interactions between unlike molecules. In addition, CED values can be transformed into Hildebrand solubility parameters (δ), defined as the square root of the CED,

$$\delta = (\mathrm{CED})^{0.5} = (\Delta E_v/V_m)^{0.5} \quad (1)$$

where ΔE_v is the energy of vaporization and V_m the molar volume.

Solubility parameters are widely used to describe the cohesive forces within materials and have been used to describe many physical properties of a material and predict interactions between materials.[12−14] The use of solubility parameters to predict solubility/miscibility is attractive and can be applied to low molecular weight materials and polymers. Solubility parameters can be evaluated by solubility studies of test materials in solvents of known solubility parameter, from refractive index values by using inverse gas chromatography, from heat of vaporization data (not suitable for many polymers), or by calculation using group contribution methods. The group contribution method was used in this paper to calculate Hildebrand solubility parameters, since these data compare well with values obtained by other methods. For example, sulfisomidine has a solubility parameter of 25.7 $MPa^{1/2}$ calculated using Fedors group contribution method and a value of 25.9 $MPa^{1/2}$ by the peak solubility method.[15] Caffeine (anhydrous) gives a solubility parameter of 28.0 $MPa^{1/2}$ using the group contribution method,[16] 28.3 $MPa^{1/2}$ by the peak solubility method,[17] and 29.9 $MPa^{1/2}$ by dissolution calorimetric measurements.[18]

Calculation of the molar vaporization energy of a material (and ultimately its Hildebrand parameter) using the group contribution method involves the summation of molar vaporization enthalpies of structural fragments in the material. The molecular volume of the material is derived from its density and molecular weight (molecular weight/density) or it can be calculated using the volume of the molecular fragment present in the material in an additive fashion similar to the calculation of vaporization energy. This enables the solubility parameter to be calculated using eq 1. An example of the calculation of solubility

* Corresponding author. Tel: +44 (0)1274 234756. Fax: +44 (0)1274 234769. E-mail: A. C.Williams@bradford.ac.uk.
[†] University of Bradford.
[‡] Bristol-Myers Squibb.

10.1021/js9900856 CCC: $18.00
Published on Web 10/01/1999

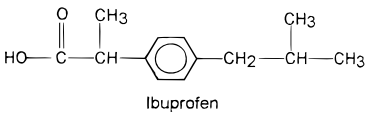

Ibuprofen

GROUP, z	^{z}U/kJ mol^{-1}	$\Sigma^{z}U$/kJ mol^{-1}	^{z}V/cm^3 mol^{-1}	$\Sigma^{z}V$/cm^3 mol^{-1}
1(COOH)	27.61	27.61	28.5	28.5
1 Phenylene	31.9	31.9	52.4	52.4
2(CH)	3.43	6.86	-1.0	-2.0
3(CH_3)	4.71	14.13	33.5	100.5
1(CH_2)	4.94	4.94	16.1	16.1
	Total	85.44	Total	195.5

$$\delta = (85440/195.5)^{1/2} = 20.9\ \text{MPa}^{1/2}$$

Figure 1—Calculation of the Hildebrand solubility parameter for ibuprofen. ^{Z}U = molar cohesive energy. ^{Z}V = molar volume. All group contributions to the molar vaporization energy and molar volume were obtained from Fedors.[19] Values apply at 25 °C.

parameters using the group contribution method is shown in Figure 1.

A short review of solid dispersion systems reported in the literature has been included in this paper and the Hildebrand solubility parameter has been calculated for the materials used. The aim was to report any incompatibilities between components in the solid dispersions and to use solubility parameters of the drug and carrier as a possible explanation, and subsequently as a predictor, for the incompatibilities. Hildebrand solubility parameters were also calculated for the materials used in this paper.

Experimental Section

Materials—The following materials were used as supplied: Ibuprofen (IB) (APS−Berk Pharmaceuticals, Eastbourne, U.K.), xylitol (XYL), sucrose, xylose, maltose, mannose, sorbitol, dextran 6, 40, 110 (Sigma-Aldrich Co. Ltd., Poole, U.K.), methanol HPLC grade (BDH Laboratory Supplies, Poole, U.K.), poloxamer 188 (Lutrol F68) (BASF plc, Cheadle Hume, U.K.), polysorbate 20, 40, 60, 80, and polyoxyethylene 40 stearate (Croda Oleochemicals, Hull, U.K.).

Preparation of Ibuprofen−Xylitol Dispersions—*Fusion Method*—IB (mp 75 °C) and XYL (mp 93 °C) were mixed at 1:1, 1:3, and 3:1 w/w to give batches of 5 g before heating to 130 °C for 1 h followed by immersion in liquid nitrogen (−196 °C) for 5 min. After solidification, samples were stored at room temperature in desiccators over P_2O_5 for 24 h before grinding and analysis by differential scanning calorimetry (DSC) and X-ray powder diffraction (XRPD).

Solvent Evaporation—Five gram batches of IB:XYL (1:1, 1:3, 3:1, and 1:9 w/w) were dissolved in the minimum volume of methanol at 40 °C. The solvent was removed under vacuum (850 mbar) using a rotary evaporator at 50 °C and 100 rpm. Samples were dried for 24 h under vacuum in a desiccator containing P_2O_5. The coevaporates formed were powders which were used without processing.

Ibuprofen−Xylitol Solubility/Miscibility Studies—Various compositions of finely ground IB and XYL (0.1−16% w/w) to give batches of 5 g were mixed in glass beakers. The mixtures were heated to 90 °C for 30 min and were stirred every 2−3 min. Visual inspections of the mixtures were made before the samples were heated to 120 °C for 30 min, again being stirred every 2−3 min. Further observations of the number of phases were made.

Miscibility Studies of Ibuprofen with other Sugars—Five gram samples of IB were heated in glass beakers to 130 °C. Sucrose (mp 190 °C), xylose (mp 158 °C), maltose (mp 128 °C), mannose (mp 135 °C), and sorbitol (mp 99 °C) were individually mixed with molten IB samples at a level of 1% w/w. The mixtures were stirred every 5 min and were maintained at 130 °C for 1 h. Five gram samples of maltose, sorbitol, and mannose were heated to 140 °C, whereupon 1% w/w IB was added to each sugar melt; the three mixtures were stirred every 5 min and were maintained at 140 °C for 1 h. This was not carried out with sucrose (mp 190 °C) and xylose (mp 158 °C) due to their high melting point and the rapid vaporization of IB above 150 °C, as confirmed by thermogravimetric analysis where a 12.1% weight loss in a sample of IB was noted between 150 °C and 200 °C (heating rate 10 °C/min). Samples were inspected for the presence of phase separation.

Preparation of Ibuprofen-Sugar Coevaporates—A 0.4 g sample of each individual sugar (sucrose, maltose, sorbitol) was dissolved in methanol at 65 °C, whereupon IB (1.6 g) was added and dissolved into the sugar solutions (1:4 w/w, sugar:drug). Solvent was removed on a rotary evaporator at 40 °C under vacuum. The coevaporates formed were transferred to a vacuum oven and evacuated to 850 mbar at room temperature overnight. The dried powders were used as produced. Coevaporates were stored in sealed vials at −18 °C for 24 h before characterization by DSC and XRPD.

Preparation of Ibuprofen−Dextran 40 Dispersion—IB (4.5 g, 90% w/w) and dextran 40 (0.5 g, 10% w/w) were dissolved in the minimum amount of a cosolvent mixture of ethanol:water (1:1 w/w) at 60 °C. The cosolvents were removed by rotary evaporation under vacuum at 50 °C. Samples were dried overnight in a vacuum oven evacuated to 850 mbar at room temperature. Samples were ground to a powder before characterization by DSC and XRPD.

Miscibility Study of Ibuprofen and Dextran 40—IB (5 g) was heated to 120 °C and 1% w/w dextran 40 was added; the melt was maintained at 120 °C for 1 h and was stirred every 5 min. Visual inspection of the melt was made to note if the dextran particles dissolved in the molten IB.

Preparation of Ibuprofen−Xylitol Dispersions incorporating Lutrol F68—Samples of IB:XYL:Lutrol F68 (1:8:1, 1:8.9:0.1, 0.5:9.4:0.1, and 0.5:9.45:0.05) were prepared to give batches of 5 g. The mixtures were heated to 110 °C for 30 min with stirring every 2−3 min before being allowed to cool to room temperature. All three components were molten at 110 °C (Lutrol F68, mp 55 °C). Samples of the melts were withdrawn using a heated Pasteur pipet (110 °C) and placed on a heated glass slide (110 °C) to be viewed under a microscope during cooling.

Miscibility Studies of Lutrol F68 with Ibuprofen and Xylitol—IB (2 g) was heated to 80 °C and XYL (2 g) to 110 °C in glass beakers, whereupon 25% w/w Lutrol F68 was mixed into the melts. Samples were stirred every 10 min and were maintained at their respective temperatures for 2 h before being allowed to cool to room temperature. The experiments were repeated using 10%, 5%, 2%, and 1% w/w Lutrol F68. Visual inspection of all the mixtures was undertaken when the samples were molten.

Miscibility Studies of Other Potential Bridging Agents with Ibuprofen and Xylitol—IB at 80 °C and XYL at 110 °C were individually mixed with other potential bridging agents, i.e., polysorbate 20, 40, 60, 80 and polyoxyethylene 40 stearate at 2% and 98% w/w to give batches of 4 g. Each mixture was heated in glass beakers to make visual assessment of the melts easier. Mixtures were maintained at their respective temperatures for 1 h with stirring every 5 min before being allowed to cool to room temperature. Visual inspection of all the mixtures was undertaken when samples were molten.

Preliminary Studies of the Interaction between Lutrol F68 and Ibuprofen—Various proportions of Lutrol F68 and IB (0−100% w/w) were mixed to give samples which had a total weight of 5 g. Each composition was heated to 90 °C for 30 min with vigorous stirring every 2−3 min before crash-cooling in liquid nitrogen. After cooling, samples were immediately transferred to a desiccator and stored over P_2O_5 for 24 h before characterization. The samples were left intact until analysis but were then ground with a mortar and pestle. All samples were characterized by DSC and XRPD. A 1:3 w/w IB:Lutrol F68 physical mix was also prepared and characterized by DSC and XRPD.

Characterization of Materials and Dispersions—*Visual Inspection*—Molten samples were viewed to assess phase separation. If components are immiscible, distinct boundaries between the constituents are expected, i.e., two liquid layers or possibly globules of one component in the continuous phase of the second component.

Thermal Analysis—Samples and starting materials were analyzed using a Perkin-Elmer Series 7 differential scanning calorimeter. Aluminum pierced and crimped pans were used in all analyses. Melting points, heat of fusion, and glass transition temperatures (T_g) quoted are the mean of three determinations,

unless otherwise stated. Temperature ranges and scan rates for each experiment are given with the results.

X-ray Powder Analysis—Samples were powdered in a mortar and pestle before X-ray analysis. X-ray patterns were obtained using a Siemens D5000 diffractometer (Stuttgart, Germany). Samples were scanned from 2° to 72° 2θ (sampling interval of 0.05°) at 1°/min using Ni-filtered Cu Kα radiation. Operating voltage and current were 40 kV and 30 mA, respectively. Diffractograms of the individual starting materials and solid dispersions were recorded.

Uniformity Study—A Philips PU 8740 UV/VIS Scanning spectrophotometer was used to analyze IB distribution within the 1:9 IB:XYL coevaporate. A calibration curve was constructed using six standard solutions of ibuprofen in methanol (range 2.0−30 μg/mL) analyzed at the λ_{max} of 221 nm. A rectilinear relationship between absorbance and ibuprofen concentration was obtained between 0.08 and 1.0 absorbance (correlation coefficient of 0.9983). XYL and methanol show no interference over the range 90−300 nm. Ten random samples (50 mg) of the unprocessed coevaporate were dissolved, filtered (0.2 μm membrane filter), and diluted with methanol to give a theoretical IB concentration in the range 0−30 μg/mL. Absorbance values for each sample at λ_{max} were converted to IB concentration and to IB concentration per gram of coevaporate using the respective weights of each random sample. The standard deviation and coefficient of variation of the IB content of the samples were used as a measure of homogeneity in the coevaporate.

Solubility Parameters and Review of Literature—Hildebrand parameters were calculated using the molar vaporization energies and molar volume values obtained by Fedors,[19] unless otherwise stated. These values are regarded as being less accurate estimations of cohesive energy[20] but are useful due to the great number of groups considered compared with other data sets. This is important as many drug molecules have complex structures.

The criterion for inclusion of solid dispersion systems in the review was the presentation of phase diagrams in the report of the systems. It was also important that the analysis of the phase diagram was by more than DSC alone, such as thermomicroscopy or capillary tube melting, so that immiscibility in the liquid state could be reported; this would not be detected by DSC analysis. Three systems were reported which did not include a phase diagram, but they were included primarily due to the evidence of liquid/liquid immiscibility by visual inspection. In these cases it was not the degree of immiscibility in the liquid state which was important but the fact that immiscibility had been identified. All the solid dispersion systems reviewed were classified into arbitrary compatibility categories based on their phase diagrams. The categories were from A (highest compatibility) to E (lowest compatibility).

Results and Discussion

Ibuprofen−Xylitol Systems—*Visual Analysis*—Visual inspection of all compositions of the IB:XYL fusion samples and samples from the solubility/miscibility study showed two distinct phases in the molten state. In the solubility/miscibility study, the mixtures at 90 °C showed particles of XYL undissolved in the IB melts at all compositions. Results indicate that the solubility of XYL in molten IB is below 0.1% w/w up to 120 °C.

DSC Studies—DSC scans (25−120 °C at 20 °C/min) of the resolidified IB:XYL fusion samples and coevaporates in Figure 2 show melting endotherms of IB (mp 75−78 °C) and XYL (mp 96−97 °C), in all compositions studied (1:1, 3:1, and 3:1 w/w). No evidence for interactions between drug and carrier is given by the DSC data, supporting the visual inspection of the melts that the drug and carrier are immiscible. The heat of fusion, corrected for dilution within the sample ($\Delta H_{f\,corr}$) and melting onset temperature of IB used in the study and those of IB in the fusion and coevaporate samples are in Table 1.

The onset of melting temperatures (Table 1) is essentially unchanged for IB in the fusion and coevaporate samples with xylitol, as compared with the starting material, again indicating little or no interaction between the drug and carrier. The melting endotherm of XYL in all dispersions with IB remained unchanged in terms of onset and peak melting temperatures compared with XYL alone. The similarity in melting points of the two components after fusion and coevaporation with the data for the starting materials indicates that no major degradation of the components occurred during the preparation procedure. This is also the case with all other systems examined in this work. The variability in $\Delta H_{f\,corr}$ (large standard deviation) shown in both coevaporate and fusion samples for IB is attributed to heterogeneity in the samples arising from the immiscibility.

X-ray Powder Analysis—XRPD diffractograms of fusion and coevaporate samples show both drug and carrier to be present in crystalline form. Peaks characteristic of IB and XYL are shown in all compositions and dispersion types. No shifts in peak positions for IB and XYL were noted, and no new peaks were observed. XRPD analysis of the resolidified fusion and coevaporate samples indicates two separate phases with no change in the crystal structures of IB and XYL. X-ray analysis gave no evidence of any interaction between the two components. Figure 3 shows diffractograms of IB, XYL, and two samples taken from the 1:3 IB:XYL coevaporate; one coevaporate sample shows peaks characteristic of XYL but none of IB, while the second sample from the same coevaporate shows the reverse. The results illustrate that IB and XYL do not

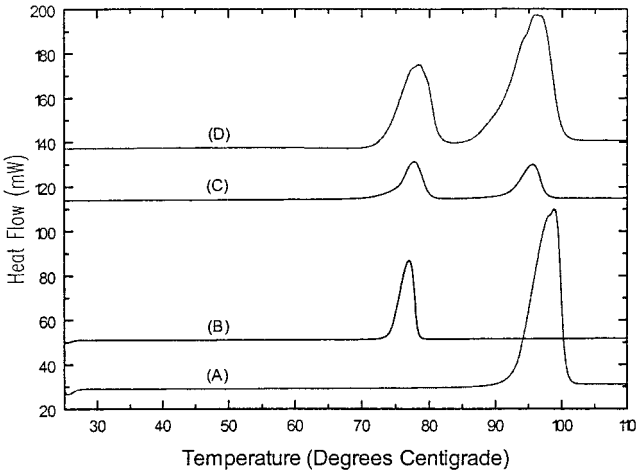

Figure 2—DSC data for xylitol alone (A), ibuprofen alone (B), 1:1 w/w IB:XYL fused sample (C), and 1:1 w/w IB:XYL coevaporate (D).

Table 1—Melting Point and Heat of Fusion of Ibuprofen in Various Solid Dispersions[a]

sample	onset of melting (°C)	melting peak (°C)	$\Delta H_{f\,corr}$ (kJ/mol)
ibuprofen	73.7 ± 0.1	75.4 ± 0.1	25.8 ± 0.2
1:1 w/w IB:XYL fusion sample	73.7 ± 0.7	78.3 ± 0.2	17.0 ± 10.0
1:3 w/w IB:XYL fusion sample	73.4 ± 0.3	76.3 ± 0.6	13.0 ± 8.0
3:1 w/w IB:XYL fusion sample	73.6 ± 0.4	79.0 ± 2.0	14.0 ± 8.0
1:1 w/w IB:XYL coevaporate	73.9 ± 0.9	77.2 ±0.5	27.0 ± 21
1:3 w/w IB:XYL coevaporate	76.0 ± 2.0	78.0 ± 2.0	33.0 ± 49
3:1 w/w IB:XYL coevaporate	74.0 ± 2.0	77.6 ± 0.8	29.5 ± 0.8
4:1 w/w IB:sucrose coevaporate	75.0 ± 2.0	80.0 ± 1.0	25.0 ± 1.0
4:1 w/w IB:maltose coevaporate	74.4 ± 0.7	78.0 ± 1.0	24.7 ± 0.1
4:1 w/w IB:sorbitol coevaporate	74.1 ± 0.4	79.6 ± 0.3	29.1 ± 0.8
9:1 w/w IB:dextran 40 coevaporate	69.7 ± 0.1	74.9 ± 0.2	19.5 ± 0.3

[a] $\Delta H_{f\,corr} = \Delta H_{obs}$ (heat of fusion of ibuprofen in sample)/theoretical % IB in sample × 100. Note: The $\Delta H_{f\,corr}$ for ibuprofen in each sample should be equivalent to the heat of fusion of the ibuprofen starting material, if ibuprofen is unaffected by the presence of excipients and the drug is uniform within the sample.

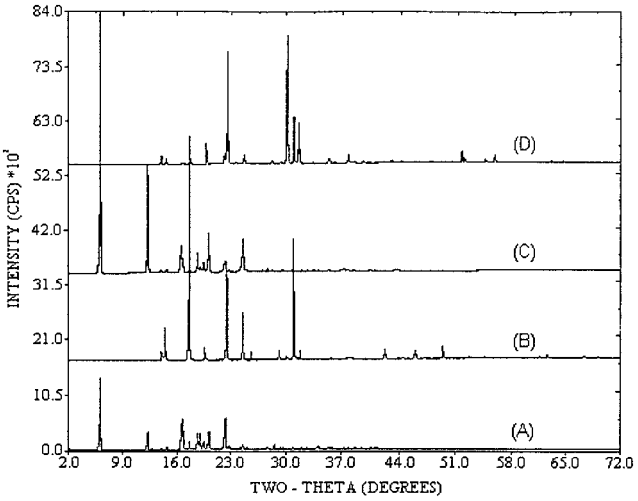

Figure 3—X-ray powder diffractograms: ibuprofen (A), xylitol (B), and IB:XYL 1:3 w/w coevaporate (C and D).

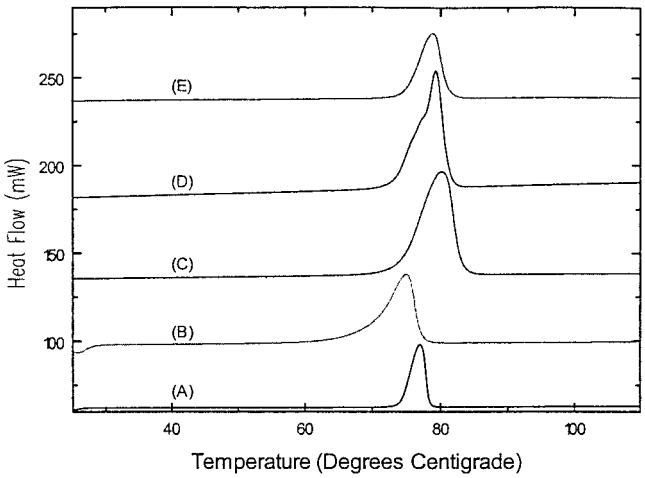

Figure 4—DSC data for ibuprofen alone (A), 1:9 w/w IB:dextran 40 coevaporate (B), 4:1 w/w IB:sorbitol (C), 4:1 w/w IB:sucrose (D), and 4:1 w/w IB:maltose (E).

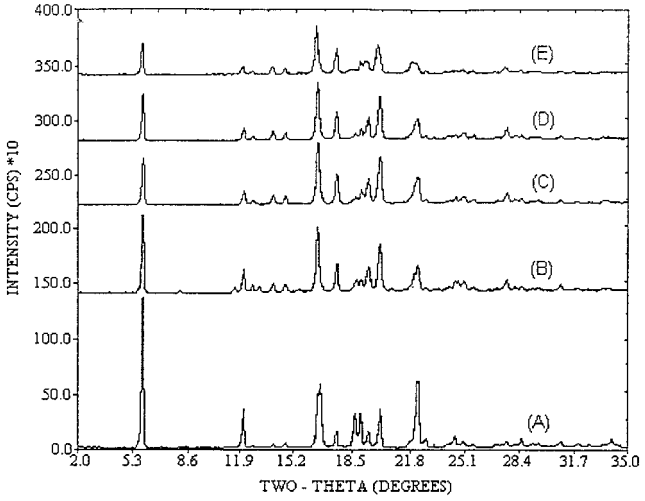

Figure 5—X-ray powder diffractograms: ibuprofen (A), IB:sucrose 4:1 w/w coevaporate (B), IB:sorbitol 1:4 w/w coevaporate (C), IB:maltose 4:1 w/w coevaporate (D), and IB:dextran 40 9:1 w/w coevaporate (E).

cocrystallize in the solvent evaporation samples, suggesting that neither drug nor carrier maintains the supersaturation of the other in solution. This would lead to the two components crystallizing out at different rates, creating isolated domains of drug and sugar.

Uniformity Study of the 1:9 IB:XYL Coevaporate—The ibuprofen content, as determined by UV spectrophotometric analysis of 10 random samples taken from the coevaporate, gave a standard deviation of ±41.9 mg/g, leading to a coefficient of variation of 64%. This shows very poor uniformity in the coevaporate at a scale of scrutiny of 50 mg (sample size). This provides further evidence of the incompatibility between IB and XYL.

Miscibility Studies of Ibuprofen with Other Sugars—*Visual Analysis*— Inspection of molten IB individually mixed with 1% w/w sucrose, xylose, and mannose showed the presence of undissolved sugar particles in all cases. Mixtures of maltose (1% w/w) with ibuprofen and sorbitol (1% w/w) with IB showed globules of sugar in the IB melts. Results show all sugars to have a solubility/miscibility below 1% w/w with ibuprofen at 130 °C. Melts of maltose, sorbitol, and mannose at 140 °C containing 1% w/w IB again show two phases with globules of IB being clearly visible.

Ibuprofen–Sugar Coevaporates—*DSC Analysis*— Coevaporates of IB:sucrose, IB:maltose, IB:sorbitol (all 4:1 w/w) were scanned from −30 to 130°C at 20 °C/min. The melting endotherm of IB was present in all three coevaporates, and the peak temperature of IB in the coevaporate remained unchanged in comparison to the starting material (Table 1). This invariance suggests that there is no disruption of the IB crystal lattice or interaction between the drug and carrier. Table 1 shows the $\Delta H_{f\,corr}$ of IB in the coevaporates to be very different from that of IB starting material. This was attributed to poor distribution of the drug in the coevaporates and correlates with the visual evidence that the sugars studied were immiscible with ibuprofen. Figure 4 shows DSC data for the IB:sugar coevaporates.

Many sugars are reported to form glasses.[21–24] No glass transition was noted over the temperature range from −30 to 130 °C for any of the sugar carriers in the coevaporates. A sample of sorbitol (5 mg) was heated in the DSC to 130 °C and maintained at this temperature for 10 min, whereupon it was cooled at 50 °C/min to −30 °C. The sample was immediately reheated in the DSC to 130 °C at 20 °C/min. A glass transition was observed at −2 °C with an associated endotherm representing the enthalpy of relaxation. Timko and Lordi[25] reported the T_g for sorbitol to be −2 °C. Maltose has been reported to have a T_g at 95 °C[24] and sucrose to have a T_g at 74 °C.[26] It must be borne in mind that glass transition temperatures can vary depending on the heating rate and with the water content of the sample.

The melting endotherms of sorbitol and maltose were not detected in the coevaporates by DSC analysis. The IB:sucrose coevaporate was not heated past the melting point of sucrose due to rapid vaporization of IB above 150 °C. The lack of melting endotherm for the sugar carriers could indicate that the sugars exist as amorphous glasses within the coevaporates. Additionally, no glass transitions were detected, probably due to the relatively low level of sugars present in the coevaporates and resulting from sampling heterogeneity due to segregation of the drug and carriers in the solid dispersions. The absence of melting endotherms for the sugar carriers is probably due to both poor homogeneity in the samples (carrier domains not sampled) and amorphous deposition of the sugars.

X-ray Powder Diffraction Studies—The X-ray diffractograms shown in Figure 5 were taken 24 h after coevaporate production. All three coevaporates produced diffraction patterns which are almost identical to each other and almost identical to that of ibuprofen starting material. The individual hydrophilic carriers cannot be easily detected

in any of the traces. Three samples of each coevaporate were analyzed by XRPD, but only one run is shown, as all the spectra produced for each coevaporate were identical. No increase in the noise level which might indicate the presence of an amorphous sugar can be seen, although the X-ray powder diffractometer may not be able to detect glassy material at a theoretical level of 20%. The XRPD data suggest that sampling and analysis of IB rich regions of the coevaporate has occurred. Segregation of the coevaporate may have occurred due to the separate crystallization of the drug and carrier.

Ibuprofen–Dextran 40 Coevaporates—*DSC Results of the Coevaporate*—Table 1 shows the melting peak temperature of IB in the dextran 40 coevaporate to be similar to the IB starting material, but the corrected heat of fusion ($\Delta H_{f\,corr}$) value is very low. The onset of melting for ibuprofen in the coevaporate is significantly lower (4 °C) compared to that of the IB starting material. The low value of $\Delta H_{f\,corr}$ is likely to be due to poor uniformity of the drug in the coevaporate; miscibility studies of IB and dextran 40 show that the two components form separate phases when mixed. The melting endotherm of IB shown in Figure 4 has a shallow onset slope which starts to rise at approximately 55 °C, this could indicate the presence of residual solvent in the coevaporate. Ibuprofen has a relatively high solubility in ethanol (1–1.5 parts ethanol[27]) and possibly forms a strong association with the solvent.

X-ray Powder Diffraction Studies—All diffractograms of the coevaporate show the crystalline structure of IB (Figure 5). One sample does show a small diffuse pattern in a diffractogram which could indicate the presence of dextran 40. X-ray analysis of dextran 40 shows it to be amorphous with no sharp diffraction peaks. Other samples do not show a significant diffuse pattern characteristic of dextran 40, indicating the absence of the carrier in the samples studied with the possibility of regions of different drug/carrier concentration being present in the coevaporate. The X-ray diffractograms show no interaction between ibuprofen and dextran 40, as no shifts in position of peaks characteristic of ibuprofen occur. No new peaks appear in any of the spectra. The intensity of peaks characteristic of IB in the dextran coevaporate are lower than the peaks in the IB starting material, even after taking into account the dilution factor of dextran 40. This could possibly be due to a decrease in IB particle size in the coevaporate or particle orientation on analysis. Several changes in relative intensities of peaks characteristic of IB are shown between the starting material and the IB–Dextran 40 coevaporate in Figure 5. Changes in crystal habit and preferred orientation of IB may have occurred in the coevaporate. If indeed this has occurred, it is debatable as to whether the presence of dextran 40 is responsible for this change. It is possible that the strong affinity of the solvent ethanol for IB has somehow modified the growth kinetics of different crystal faces on the growing IB crystals. The effect of solvent of crystallization on the morphology of IB has been shown, with needlelike crystals being produced when IB is recrystallized from hexane and more equidimensional crystals being produced when recrystallized from ethanol.[28]

Miscibility Study of Ibuprofen and Dextran 40—Inspection of the IB melt at 120 °C containing 1% w/w dextran 40 showed particles of the carbohydrate dispersed in the melt; dextran 40 is not soluble in IB under these conditions.

Ibuprofen–Xylitol Dispersions Incorporating Lutrol F68—*Microscopy*—In all cases the ternary dispersions showed two phases when molten with a dispersion of the lipophilic IB globules in the XYL continuous phase. It was noted that with the binary system of IB and XYL in the molten state, phase separation was quite distinct with two completely separate regions. Vigorous stirring of the melts created globules of one phase dispersed in the continuous phase of the second component. The dispersion was not stable and reverted to separate phases within a matter of seconds on discontinuation of stirring. The incorporation of Lutrol F68 caused visible "macroglobules" of IB in the XYL continuous phase. The dispersion of globules was relatively stable in comparison to the binary system of IB: XYL, as discontinuation of stirring did not result in complete phase separation of IB and XYL. Results suggest that the addition of Lutrol F68 has lowered the interfacial tension between IB and XYL. Microscopy highlighted the two phases and showed separate crystallization of the phases, with xylitol crystallizing first in all sample compositions. The IB phase crystallized 2–3 h after the crystallization of XYL.

DSC Analysis—Many of the samples taken from the resolidified mixtures of various ratios of drug:carrier: bridging agent only showed the melting endotherm of XYL (onset, 92 ± 1 °C, $n = 5$) when analyzed by DSC (10–110 °C at 5 °C/min). The possibility that IB and Lutrol F68 were amorphous in the dispersion was disproved with subsequent XRPD experiments and by preliminary interaction studies. The absence of melting endotherms for Lutrol F68 and especially for IB was attributed to the phase separation and heterogeneity observed by microscopy. A sample of the 1:1:8 IB:Lutrol F68:XYL dispersion showed a melting endotherm of 44 °C (onset, 39 °C), which did not correspond to the melting points of any of the components; melting onset of Lutrol F68 is 52.0 ± 0.5 °C (Figure 5). This suggested an interaction between components in the sample. This was further investigated by studying dispersions of Lutrol F68 with IB produced by the fusion method.

X-ray Powder Analysis—Diffractograms of all resolidified ternary mixtures showed heterogeneity in the samples with two phases present. Peaks characteristic of IB and XYL were identified. The absence of any shifts in peak positions or the presence of new peaks indicated no change in the crystal structures of IB or XYL in any of the dispersions. XRPD did not detect any peaks characteristic of Lutrol F68 in any of the samples.

Miscibility Studies—*Lutrol F68 with IB and XYL*—Inspection indicated that at least 25% w/w Lutrol F68 dissolved in IB at 80 °C, whereas a 1% w/w Lutrol F68 in xylitol mix showed a fine dispersion of Lutrol F68 at 110 °C.

Polysorbate 20, 40, 60, 80 and Polyoxyethylene 40 Stearate with IB and XYL—Inspection of the melts (80 °C) showed IB to be miscible with all of the bridging agents at 2% and 98% w/w, while XYL showed two phases with every bridging agent at the 2% and 98% w/w levels (110 °C).

Preliminary Interaction Studies of Ibuprofen and Lutrol F68—The resolidified IB:Lutrol F68 samples were analyzed by DSC from 0 to 120 °C at 5 °C/min. A binary phase diagram produced from the DSC curves of the dispersions showed the system to be a simple eutectic with a eutectic composition between 65 and 70% w/w Lutrol F68 (approximate mole ratio 20:1, IB:Lutrol F68) and a eutectic melting point of 37 ± 2 °C (onset temperature). This eutectic behavior between IB and Lutrol F68 has been documented previously.[29] Figure 6 shows DSC data on the physical mix and fusion samples of the IB:Lutrol F68 system. It can be seen that both the physical mix and fusion sample have a melting endotherm at approximately 37 °C. It appears that eutectic formation can occur by simply mixing. Three samples of the 1:3 w/w (slight excess of Lutrol F68) physical mix were analyzed by DSC and all show the same single melting endotherm at 39.6 ± 0.3 °C (onset temperature).

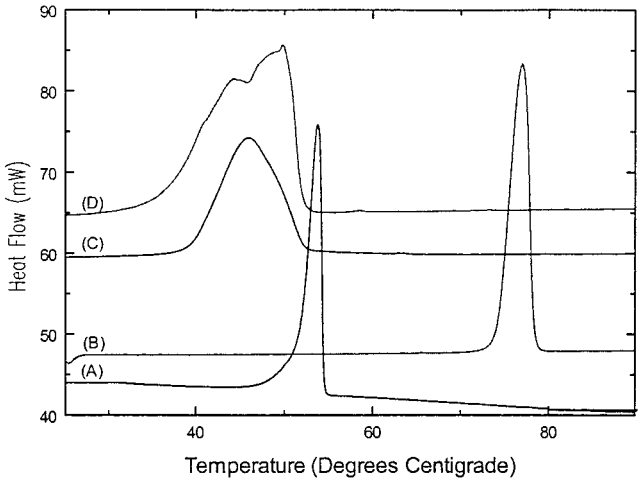

Figure 6—DSC analysis of Lutrol F68 alone (A), ibuprofen alone (B), 1:3 w/w IB:Lutrol F68 physical mixture (C), and 1:3 w/w IB:Lutrol F68 fused sample (D).

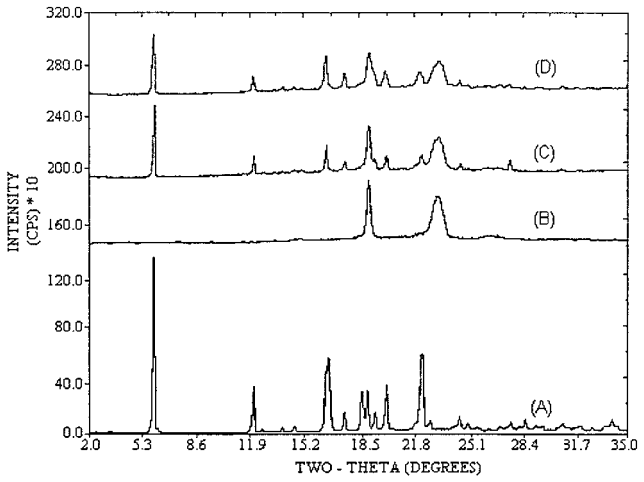

Figure 7—X-ray powder diffractograms: ibuprofen (A), Lutrol F68 (B), IB: Lutrol F68 1:3 w/w ground mixture (C), and IB:Lutrol F68 1:3 w/w fusion sample (D).

XRPD Analysis—Diffractograms of the IB:Lutrol F68 solid dispersions indicate IB to be crystalline and Lutrol F68 to be semicrystalline. Figure 7 shows traces of IB, Lutrol F68, a 1:3 w/w IB–Lutrol F68 physical mix, and fusion sample at 25 °C. Peaks characteristic of IB and Lutrol F68 can be seen in both the physical mix and fusion sample. The diffractograms of the physical mix and fusion samples in Figure 7 show that fusion of the components does not cause interactions between the drug and carrier on a bulk scale at 25 °C; crystal surface interactions may occur undetected by XRPD. Little change in crystallinity occurs on fusing the drug and carrier, as illustrated by the similar peak intensities in the traces of the physical mix and fusion sample (Figure 7). Further analysis of XRPD data from the binary system shows no shifts in peak position for IB or Lutrol F68, suggesting no changes in their bulk crystal structures. No evidence for solid solution formation between 10 and 90% w/w Lutrol F68 was found.

Solubility Parameters—Table 3 gives a list of drug/carrier systems which have been used in this and other selected studies in an attempt to produce solid dispersions of poorly water-soluble drugs. A brief description of each system, the solubility parameters of the components, and the difference in solubility parameters of the two materials are given in an attempt to identify a link between immiscibility problems and differences in the solubility parameter. The systems have been categorized in terms of miscibility, using the classification system in Table 2.

Several of the drug/carrier systems in Table 3 show a strong link between differences in solubility parameter and incompatibility. IB, tolbutamide, and nifedipine show interactions with carriers that possess similar solubility parameters (differences ranging from 1.6 to 7.0 $MPa^{1/2}$) and immiscibility problems with carriers where the difference in solubility parameter is above 10 $MPa^{1/2}$ (differences ranging from 10.8 to 18.0 $MPa^{1/2}$). The systems in Table 3 have been classified into arbitrary groups. Category B contains several different types of phase diagram, but these cannot be differentiated further by studying $\Delta\delta$. For example, 70% w/w of phenobarbital dissolves in citric acid at its melting point and $\Delta\delta$ is 4.3 $MPa^{1/2}$. Within the same category naproxen shows negligible solubility in PEG 4000 at its melting point but $\Delta\delta$ is only 3.5 $MPa^{1/2}$. From the data in Table 3 it is difficult to predict what type of phase diagram will result with drug/carrier systems where the $\Delta\delta$ is below 7.5 $MPa^{1/2}$. However, Table 3 does show a general trend in that systems with a $\Delta\delta$ ranging from 1.6 to 7.5 $MPa^{1/2}$ show complete miscibility when molten; systems with a $\Delta\delta$ from 7.4 to 15.0 $MPa^{1/2}$ show some sign of immiscibility in the liquid state, and systems with a $\Delta\delta$ above 15.9 exhibit total immiscibility over the entire composition range. The lack of a clear link between the type of phase diagram and $\Delta\delta$ where $\Delta\delta$ is relatively small (i.e. systems in category B) may relate to the accuracy of the solubility parameters quoted, especially with polymer carriers. It is also considered that Fedors' values of group contributions are less accurate than other data sets.[20] Further, Hildebrand parameters do not detail types of interactions in materials, unlike Hansen partial solubility parameters, which give the relative strengths of the dispersion forces, polar forces, and hydrogen bonding forces present in the material. If Hansen parameters were compared between drug and carrier, clearer links between partial solubility parameters and degree of miscibility may be established. The lack of a clear relationship between phase diagrams and $\Delta\delta$ may also relate to the fact that materials may exhibit two or more solubility parameters in an effort to adapt to their environment,[39] which is not accounted for with Hildebrand parameters. This can occur with materials that possess functional groups capable of hydrogen bonding; this "chameleonic effect" has been reported with sulfamethyoxypyridazine in solvents of vary-

Table 2—Classification of Miscibility

category	type of phase diagram
A	Both components completely miscible at all compositions in the liquid state. Large degree of solid/solid solubility (above 5% w/w). Complex formation.
B	Both components completely miscible at all compositions in the liquid state. Eutectic systems (immeasurable solid solution formation), where there is substantial solubility of one component in the second component at its melting point. Systems where there is a melting point depression of only the highest melting point component but negligible solubility of this material in the second component at its melting point.
C	Both components completely miscible at all compositions in the liquid state. Limited or no solubility of component A in B or B in A below melting point of either component.
D	Some degree of immiscibility when both components are in the liquid state.
E	Complete immiscibility at all proportions when both components are molten.

Table 3—Solubility Parameters and Classification of Solid Dispersions in Terms of Miscibility

drug/carrier system (category)	description	δ (MPa)$^{1/2}$	$\Delta\delta$[a]	ref
ibuprofen/PVP (A)	IB forms a 1:1 drug:polymer complex in the solid state (XRPD and DSC studies).	20.9/22.5[b]	1.6	Najib et al.[30]
chlorthalidone/urea (B)	Forms a eutectic system. Eutectic composition contained 35% w/w chlorthalidone.	32.6/38.5	5.9	Bloch et al.[31]
diazepam/PEG 4000 (B)	Forms a eutectic system. Eutectic composition contained 17% w/w diazepam.	27.4/19.9[c]	7.5	Anastasiadou et al.[32]
famotidine/xylitol (B)	Forms a eutectic system. Eutectic composition contained ca. 2.4% w/w famotidine.	29.6/37.1	7.5	Mummaneni and Vasavada[33]
flurbiprofen/PEG 400 and 6000 (B)	Forms a eutectic system by physical mixing, coevaporation, and comelting. Eutectic composition contained 35% w/w flurbiprofen with PEG 4000 and 33% w/w with PEG 6000.	23.7/19.9,[c] 23.7/19.8[c]	3.8, 3.9	Lacoulonche et al.[34]
griseofulvin/PEG 2000 (B)	Melting point depression of drug (liquidus curve), but not of PEG (solidus curve). Negligible solubility of drug in PEG at its mp. Liquidus curve meets solidus curve at 0% drug and mp of PEG. The rising liquidus curve with increasing amount of drug analogous to the solubility of the drug in molten PEG at various temperatures.	23.9/20.1[c]	3.8	Kaur et al.[35]
griseofulvin/polyoxyethylene 40 stearate (POES) (B)	Melting point depression of drug (liquidus curve), but not of POES (solidus curve). Negligible solubility of drug in POES at its mp. Liquidus curve meets solidus curve at 0% drug and mp of POES. The rising liquidus curve with increasing amount of drug analogous to the solubility of the drug in molten POES at various temperatures.	23.9/19.8[c]	4.1	Kaur et al.[35]
ibuprofen/Lutrol F68 (B)	Forms a eutectic system. Eutectic composition contained 30–35% w/w ibuprofen.	20.9/19.0[d]	1.9	Reported in this paper. Hawley et al.[29]
naproxen/PEG 4000 and 6000 (B)	Melting point depression of drug (liquidus curve), but not of PEG (solidus curve). Negligible solubility of drug in PEG at its mp. Liquidus curve meets solidus curve at 0% drug and mp of PEG. The rising liquidus curve with increasing amount of drug analogous to the solubility of the drug in molten PEG at various temperatures.	23.4/19.9, 23.4/19.8	3.5, 3.6	Mura et al.[36]
nifedipine/ethylurea ETU (B)	Melting point depression of drug (liquidus curve), but not of ETU (solidus curve). Negligible solubility of drug in ETU at its mp. Liquidus curve meets solidus curve at 0% drug and mp of ETU. The rising liquidus curve with increasing amount of drug analogous to the solubility of the drug in molten ETU at various temperatures	24.8/28.9	4.1	Suzuki and Sunada[3]
nifedipine/nicotinamide (B)	Forms a eutectic system. Eutectic composition contained 25% w/w nifedipine.	24.8/31.8	7.0	Suzuki and Sunada[3]
nifedipine/PEG 6000 (B)	Melting point depression of drug (liquidus curve) but not of PEG (solidus curve). Negligible solubility of drug in PEG at its mp. Liquidus curve meets solidus curve at 0% drug and mp of PEG. The rising liquidus curve with increasing amount of drug analogous to the solubility of the drug in molten PEG at various temperatures.	24.8/19.8[c]	5.0	Suzuki and Sunada[3]
phenobarbital/citric acid (B)	60–70% w/w phenobarbital is soluble in citric acid at its melting point. All mixtures show a single homogeneous phase when molten.	29.5/33.8	4.3	Timko and Lordi[37]
tolbutamide/PEG 2000 (B)	Melting point depression of drug (liquidus curve) but not of PEG (solidus curve). Negligible solubility of drug in PEG at its mp. Liquidus curve meets solidus curve at 0% drug and mp of PEG. The rising liquidus curve with increasing amount of drug analogous to the solubility of the drug in molten PEG.	23.2[e]/20.1[c]	3.1	Kaur et al.[35]
tolbutamide/polyoxyethylene 40 stearate (B)	10% w/w tolbutamide dissolves in POES at its melting point; liquidus curve (drug melting) meets solidus curve (POES melting) at 10% w/w tolbutamide and mp of POES. The rising liquidus curve with increasing amount of drug analogous to the solubility of the drug in molten POES at various temperatures. No mp depression of POES at any composition.	23.2[e]/19.8[c]	3.4	Kaur et al.[35]
acetaminophen/dextrose (D)	Liquid immiscibility over large composition range in phase diagram. Visual inspection of melts shows two phases. Two T_gs representing glass solution of carrier in drug in midrange of phase diagram, corresponds to two phases when both components are molten. Single T_g at low and high % drug; single phase when drug and carrier are molten.	30.8/43.1	12.3	Timko and Lordi[25]
acetaminophen/sorbitol (D)	Liquid immiscibility over large composition range in phase diagram. Visual inspection of melts shows two phases. Two T_gs representing glass solution of drug in carrier and glass solution of drug in carrier and glass solution of carrier in drug in midrange of phase diagram; corresponds to two phases when both components are molten. Single T_g at low and high % drug, single phase when drug and carrier are molten.	30.8/38.2	7.4	Timko and Lordi[25]
nifedipine/erythritol[f] (D)	At 25% w/w nifedipine, two liquid phases identified when components are molten.	24.8/35.6	10.8	Suzuki and Sunada[3]
nifedipine/urea[f] (D)	At 25% w/w nifedipine, two liquid phases identified when components are molten.	24.8/38.5	13.7	Suzuki and Sunada[3]
nifedipine/xylitol[f] (D)	At 25% w/w nifedipine, two liquid phases identified when components are molten.	24.8/37.1	12.3	Suzuki and Sunada[3]
phenobarbital/sorbitol (D)	Liquid immiscibility over large composition range in phase diagram. Visual inspection of melts shows two phases. Two T_gs representing glass solution of drug in carrier and glass solution of carrier in drug in midrange of phase diagram; corresponds to two phases when both components are molten. Single T_g at low and high % drug; single phase when drug and carrier are molten.	29.5/38.2	8.7	Timko and Lordi[25]
tolbutamide/mannitol (D)	Eutectic formation. Eutectic composition contained 94% w/w tolbutamide. Formation of two liquid phases at 40 and 80% w/w mannitol above melting point of mannitol.	23.2[e]/38.2	15.0	El-Banna et al.[11]
hexobarbital/dextrose (F)	Liquid/liquid immiscibility over complete composition range. Visual inspection of melts. Two T_gs representing pure drug and pure carrier were present over entire composition range.	27.2/43.1	15.9	Timko and Lordi[25]
ibuprofen/maltose (F)	Immiscible when both components are molten at 1% and 99% w/w; visual inspection of melts.	20.9/38.9	18.0	reported in this paper

Table 3 (Continued)

drug/carrier system (category)	description	δ (MPa)$^{1/2}$	$\Delta\delta$[a]	ref
ibuprofen/sorbitol (F)	Immiscible when both components are molten at 1% and 99% w/w, visual inspection of melts.	20.9/38.2	17.3	reported in this paper
ibuprofen/xylitol (F)	Immiscible when both components are molten at 25% w/w, 50% w/w, 75% w/w and 99.9% w/w, ibuprofen	20.9/37.1	16.2	reported in this paper

[a] $\Delta\delta$ is difference in solubility parameters between drug and carrier. [b] The molar group contributions to polymer cohesive energies compiled by Van Krevelen and Hoftyzer[38] were used. These tables contain no value for the amide group in the molecule, so Fedors' value[19] for the group was used. [c] The Hildebrand solubility parameter was calculated using entire molecule. Group molar attraction constants of Van Krevelen and Hoftyzer[38] were used. [d] The Hildebrand solubility parameter for Lutrol (polyoxyethylene–polyoxypropylene–polyoxyethylene block copolymer) was calculated using molar group contributions to polymer cohesive energies compiled by Van Krevelen and Hoftyzer.[38] [e] A value for the contribution of the $-SO_2-$ group to the molar vaporization energy of the molecule was obtained from Martin et al.[15] Values for the other groups within the molecule were obtained from tables compiled by Fedors.[19] [f] Drug/carrier systems could belong to category E as the degree of immiscibility in the liquid state is not known.

ing polarity, with the drug showing solubility maxima in solvents with Hildebrand solubility parameters of 30.9 MPa$^{1/2}$ (lower solubility peak) and 20.9 MPa$^{1/2}$ (higher solubility peak). The Hildebrand solubility parameter of sulfamethoxypyridazine was calculated at 25.0 MPa$^{1/2}$ using Fedors' group contribution method.[39] Benzoic acid also shows a solubility parameter of 26.9 MPa$^{1/2}$ in highly polar solvents and 23.1 MPa$^{1/2}$ in less polar mixtures;[39] the calculated value was 24.4 MPa$^{1/2}$. Many of the drugs in Table 3 possess several polar and hydrogen bonding groups within the molecule and are probably capable of interacting with different materials in a number of different ways. The donor−acceptor capacity of hydrogen-bonding groups in drug and carrier must be considered to maximize interaction between the two materials. One further consideration when using solubility parameters is that δ may modify with temperature. It is possible that different materials will have solubility parameters which change to varying degrees with a change in temperature; these differences may become significant at high temperatures and may play a role in high melting point drug/carrier systems, for example, phenobarbital (mp 174−178 °C) and citric acid (mp 152−156 °C). Crystallinity can also have an effect on solubility parameters, as was shown by Egawa et al.,[40] where amorphous cefalexin was shown to have higher partial solubility parameters compared to a crystalline sample.

However, despite the limitations of the approach, solubility parameters may provide a simple and generic capability for rational selection of carriers in the preparation of solid dispersions. From the data generated in the present study, miscibility was shown between ibuprofen and Lutrol F68, where solubility parameters differed only by 1.9 and where a eutectic system was formed. Similarly, from the literature, ibuprofen/PVP systems where $\Delta\delta$ is only 1.6 were also completely miscible.[30] In contrast, our data have also demonstrated immiscibility where solubility parameters are markedly different; ibuprofen with maltose, sorbitol, and xylitol did not form solid dispersions and $\Delta\delta$ values were 18.0, 17.3, and 16.2, respectively. These data thus appear to support the validity of using solubility parameter differences as a tool for judicial selection of carrier components. Subsequent analysis and further refinement of this approach would need to address other factors such as crystallization inhibition by the excipient.

Conclusion

Ibuprofen has been shown to be incompatible with many sugar carriers when attempting to form solid dispersions. The coevaporate and fusion samples of ibuprofen with xylitol and the other sugar carriers show a decreased uniformity of the drug in the carrier compared to simple mixing. Both coevaporates and fusion samples must be powdered and blended to get a homogeneous dispersion. The mixing of ibuprofen with noninteracting sugar carriers may increase the drug's dissolution rate to a small extent, but overall it is probable that a drug and carrier combination where interactions between components occur will show a faster dissolution rate of the hydrophobic drug in aqueous medium. The use of bridging agents to facilitate dispersion of ibuprofen into xylitol did not prove successful, since none of the bridging agents mixed with xylitol. All bridging agents were miscible with ibuprofen.

This paper has highlighted a trend in terms of increasing degrees of immiscibility with increasing difference in solubility parameter between drug and carrier. The use of Hildebrand solubility parameters to predict compatibility has been reported by Suzuki and Sunada[41] and was found useful for selecting a suitable polymer as a component of combined carriers in solid dispersions of nifedipine. The Hildebrand solubility parameters used in this paper are relatively quick to calculate using group contribution methods and have the advantage that data for different structural groups are readily available, enabling calculation of solubility parameters for many complex drug molecules. However, it has been highlighted that the use of Hildebrand parameters in predicting accurately the phase diagram and specific level of interaction between drugs and carriers is limited. Several reasons for the observed anomalies have been discussed, including the fact that Hildebrand parameters give the overall cohesive energy in the materials but less information on the relative strengths of the various types of forces present (dispersion, polar, and hydrogen bonding). On this basis improved predictive qualities can be obtained using the Hansen partial solubility parameters (δ_d, δ_p, and δ_h). One practical problem of calculating Hansen parameters using group contribution methods is the limited data available on structural groups, thus causing difficulties for complex drug molecules. A database of partial solubility parameters for carriers and the determination of the contribution to partial solubility parameters of more structural groups found in drug molecules may enable prediction of compatible carriers which form strong associations with the drug, resulting in anticipating solid dispersion systems with fast drug dissolution rates.

References and Notes

1. Danjo, K.; Nakata, T.; Otsuka, A. Preparation and Dissolution of Ethenzamide Solid Dispersions using Various Sugars as Dispersion Carriers. *Chem. Pharm. Bull.* **1997**, *45*, 5 (11), 1840−1844.
2. Save, T.; Venkitachalam, P. Studies on Solid Dispersions of Nifedipine. *Drug Dev. Ind. Pharm.* **1992**, *18* (15), 1663−1679.
3. Suzuki, H.; Sunada, H. Comparison of Nicotinamide, Ethylurea and Polyethylene Glycol as Carriers for Nifedipine Solid Dispersion Systems. *Chem. Pharm. Bull.* **1997**, *45*, 5 (10), 1688−1693.

4. Akbuga, J.; Gursoy, A.; Kendi, E. The Preparation and Stability of Fast Release Furosemide-PVP Solid Dispersion. *Drug Dev. Ind. Pharm.* **1988**, *14* (10), 1439−1464.
5. Chiou, W. L.; Reigelman, S. Preparation and Dissolution Characteristics of Several Fast-Release Solid Dispersions of Griseofulvin. *J. Pharm. Sci.* **1969**, *58*, 1505−1509.
6. Kaur, R.; Grant, D. J. W.; Eaves, T. Comparison of Polyethylene Glycol and Polyoxyethylene Stearate as Excipients for Solid Dispersion Systems of Griseofulvin and Tolbutamide II: Dissolution and Solubility Studies. *J. Pharm. Sci.* **1980**, *69*, 1321−1326.
7. McGinity, J. W.; Maincent, P.; Steinfink, H. Crystallinity and Dissolution Rate of Tolbutamide Solid Dispersions prepared by the Melt Method. *J. Pharm. Sci.* **1984**, *73*, 1441−1444.
8. Ford, J. L.; Rubinstein, M. H. Preparation, Properties and Aging of Tablets prepared from the Chlorpropamide-Urea Solid Dispersion. *Int. J. Pharm.* **1981**, *8*, 311−322.
9. Sugimoto, I.; Kuchiki, A.; Nakagawa, H. Stability of Nifedipine-Poly(vinylpyrrolidone) Coprecipitate. *Chem. Pharm. Bull.* **1981**, *29* (6), 1715−1723.
10. Kanig, J. L. Properties of Fused Mannitol in Compressed Tablets. *J. Pharm. Sci.* **1964**, *53*, 188−192.
11. El-Banna, H. M.; Daabis, N. A.; Mortada, L. M.; Abd-Elfattah, S. Physicochemical Study of Drug Binary Systems Part 3: Tolbutamide-Urea and Tolbutamide−Mannitol Systems. *Pharmazie* **1975**, *30*, 788−792.
12. Rowe, R. C. Adhesion of Film Coatings to Tablet Surfaces − a Theoretical Approach based on Solubility Parameters. *Int. J. Pharm.* **1988**, *41*, 219−222.
13. Rowe, R. C. Interactions in Coloured Powders and Tablet Formulations: a Theoretical Approached based on Solubility Parameters. *Int. J. Pharm.* **1989**, *53*, 47−51.
14. Rowe, R. C. Polar/Nonpolar Interactions in the Granulation of Organic Substrates with Polymer Binding Agents. *Int. J. Pharm.* **1989**, *56*, 117−124.
15. Martin, A.; Wu, P. L.; Valesquez, T. Extended Hildebrand Solubility Approach: Sulfonamides in Binary and Ternary Solvents. *J. Pharm. Sci.* **1985**, *74* (3), 277−282.
16. Ticehurst, M. D. Characterisation of the Surface Energetics of Pharmaceutical Powders by Inverse Gas Chromatography. Ph.D. Thesis 1994, University of Bradford, U.K.
17. Adjei, A.; Newburger, J.; Martin, A. Extended Hildebrand Approach: Solubility of Caffeine in Dioxane-Water Mixtures. *J. Pharm. Sci.* **1980**, *69* (6), 659−661.
18. Rey-Mermet, C.; Ruelle, P.; Nam-Tran, H.; Buchmann, M.; Kesselring, U. W. Significance of Partial and Total Cohesion Parameters of Pharmaceutical Solids determined from Dissolution Calorimetric Measurements. *Pharm. Res.* **1991**, *8* (5), 636−642.
19. Fedors, R. A Method for Estimating both the Solubility Parameters and Molar Volumes of Liquids. *Polym. Eng. Sci.* **1974**, *14* (2), 147−154.
20. Barton, A. F. M. *Handbook of Solubility Parameters and other Cohesion Parameters*, 4th ed.; CRC Press Inc.: Boca Raton, FL, 1988; p 62.
21. Roos, R.; Karel, M. Water and Molecular Weight Effects on Glass Transitions in Amorphous Carbohydrates and Carbohydrate Solutions. *J. Food Sci.* **1991**, *56* (6), 1676−1681.
22. Roos, R. Melting and Glass Transitions of Low Molecular Weight Carbohydrates. *Carbohydr. Res.* **1993**, *238*, 39−48.
23. Finegold, L.; Franks, F.; Hatley, R. H. M. Glass/Rubber Transitions and Heat Capacities of Binary Sugar Blends. *J. Chem. Soc., Faraday Trans. 1* **1989**, *85* (9), 2945−2951.
24. Orford, P. D.; Parker, R.; Ring, S. G. Aspects of the Glass Transition Behaviour of Mixtures of Carbohydrates of Low Molecular Weight. *Carbohydr. Res.* **1990**, *196*, 11−18.
25. Timko, R. J.; Lordi, N. G. Thermal Analysis Studies of Glass Dispersion Systems. *Drug Dev. Ind. Pharm.* **1984**, *10* (3), 425−451.
26. Saleki-Gerhardt, A.; Zografi, G. Non-Isothermal Crystallization of Sucrose from the Amorphous State. *Pharm. Res.* **1994**, *11* (8), 1166−1173.
27. *Clark's Isolation and Identification of Drugs*, 2nd ed.; Moffat, A. C., Jackson, J. V., Moss, M. S., Widdop, B., Eds.; The Pharmaceutical Press: London, 1986; p 677.
28. Bunyan, J. M. E.; Shankland, N.; Sheen, D. B. Solvent Effects on the Morphology of Ibuprofen. *Particle Design via Crystallisation* AIChE Symp. Series, **1991**, *87* (284), 44−57.
29. Hawley, A. R.; Rowley, G.; Lough, W. J.; Chatham, S. Physical and Chemical Characterisation of Thermosoftened Bases for Molten Filled Hard Gelatin Capsule Formulations. *Drug Dev. Ind. Pharm.* **1992**, *18* (16), 1719−1739.
30. Najib, N. M.; El-Hinnawi, M. A.; Suleiman, M. S. Physicochemical Characterisation of Ibuprofen-Poly(vinylpyrrolidone) Dispersions. *Int. J. Pharm.* **1988**, *45*, 139−144.
31. Bloch, D. W.; Elegakey, M. A.; Speiser, P. P. Solid Dispersion of Chlorthalidone in Urea Phase Diagram and Dissolution Characteristics. *Pharm. Acta Helv.* **1982**, *57*, 231−235.
32. Anastasiadou, C.; Henry, S.; Legendre, B.; Souleau, C.; Duchene, D. Solid Dispersions: Comparison of Prepared Melts and Coprecipitates of Diazepam and Polyoxyethylene Glycol 4000. *Drug Dev. Ind. Pharm.* **1983**, *9*, 103−115.
33. Mummaneni, V,; Vasavada, R. C. Solubilization and Dissolution of Famotidine from Solid Glass Dispersions of Xylitol. *Int. J. Pharm.* **1990**, *66*, 71−77.
34. Lacoulonche, F.; Chauvet, A.; Masse, J.; Egea, M. A.; Garcia, M. L. An Investigation of FB Interactions with Poly(ethylene glycol) 6000, Poly(ethylene glycol) 4000 and Poly-ϵ-caprolactone by Thermoanalytical and Spectroscopic Methods and Modeling. *J. Pharm. Sci.* **1998**, *87* (5), 543−551.
35. Kaur, R.; Grant, D. J. W.: Eaves, T. Comparison of Polyethylene Glycol and Polyoxyethylene Stearate as Excipients for Solid Dispersion Systems of Griseofulvin and Tolbutamide I: Phase Equilibra. *J. Pharm. Sci.* **1980**, *69* (11), 1317−1320.
36. Mura, P.; Manderioli, A.; Bramanti, G.; Ceccarelli, L. Properties of Solid Dispersions of Naproxen in Various Polyethylene Glycols. *Drug Dev. Ind. Pharm.* **1996**, *22*, 909−916.
37. Timko, R. J.; Lordi, N. G. Thermal Analysis Studies of Glass Dispersion Systems. *Drug Dev. Ind. Pharm.* **1984**, *10* (3), 425−451.
38. Van Krevelen, D. W.; Hoftyzer, P. J. Properties of Polymers: Their Estimation and Correlation with Chemical Structure, 2nd ed.; Elsevier: Amsterdam, 1976; pp 129−159.
39. Escalera, J. B.; Bustamante, P.; Martin, A. Predicting the Solubility of Drugs in Solvent Mixtures: Multiple Solubility Maxima and the Chameleonic Effect. *J. Pharm. Pharmacol.* **1994**, *46*, 172−176.
40. Egawa, H.; Maeda, S.; Yonemochi, E.; Oguchi, T.; Yamamoto, K.; Nakai, Y. Solubility Parameter and Dissolution Behavior of Cefalexin Powders with Different Crystallinity. *Chem. Pharm. Bull.* **1992**, *40*, 819−820.
41. Suzuki, H.; Sunada, H. Influence of Water-Soluble Polymers on the Dissolution of Nifedipine Solid Dispersions with Combined Carriers. *Chem. Pharm. Bull.* **1998**, *46*, 6 (3), 482−487.

Acknowledgments

D.J.G. thanks the BBSRC and Bristol-Myers Squibb Pharmaceutical Research Institute for Financial Support. The authors also thank APS−Berk Pharmaceuticals (Eastbourne, England) for donating ibuprofen, BASF plc (Cheadle Hulme, U.K.) for the polysorbates and polyoxyethylene 40 Stearate, and Croda Oleochemicals (Hull, U.K.) for the Lutrol F68.

JS9900856